Correlation between multiple chemical modification strategies on graphene or graphite and physical / electrical properties

Thibaut Lalire, Belkacem Otazaghine, Aurélie Taguet, Claire Longuet

Correlation between multiple chemical modification strategies on graphene or graphite and physical / electrical properties

Authors

Thibaut LALIRE*, Belkacem OTAZAGHINE*, Aurélie TAGUET, Claire LONGUET

Polymers Composites and Hybrids (PCH), IMT Mines Ales, Ales, France

Abstract

Chemical modifications of carbon based materials are often used to improve their dispersion in polymer matrix and increase the nanocomposite electrical properties. This work concerned the control of graphene and graphite physical and chemical structure thanks to different chemical modification (oxidation, copolymer functionalization and reduction). This article exposes a complete study of different chemical modifications impact on graphene and graphite microstructure, chemical structure, and its relative electrical property. A first oxidation step by Hummers or nitric acid method was necessary to further graft a copolymer of methyl methacrylate and hydroxyethyl methacrylate via a versatile "grafting onto" covalent functionalization. Hummers' and nitric acid methods were considered as strong and soft oxidation treatments, respectively. Reduction steps were also performed using hydrazine or thermal treatments to recover high electrical conductivity. Chemical modifications of graphene and graphite were characterized by X-ray diffraction, Raman spectroscopy, thermogravimetric analysis, Fourier transform infrared spectroscopy and pyrolysis–gas chromatography–mass spectrometry. Moreover, a new method for the electrical measurement of the modified particles is presented in this work. This measurement requires adhesive tape and an electrical circuit with a diode using the four probes protocol, it allows the evaluation of the electrical conductivity of the graphene and graphite samples in powder state. Finally, the electrical resistances of the different graphene and graphite submitted to all the chemical treatments are reported.

Graphical abstract

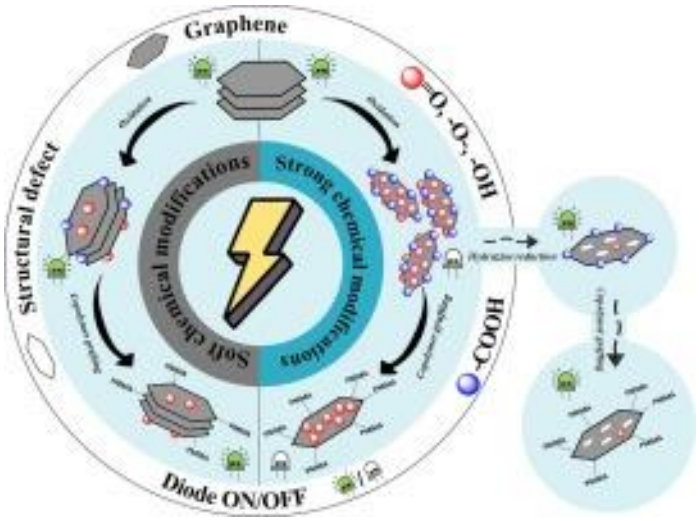

Keywords

Graphene; Graphite; Nanocomposite; Electrical conductivity; Functionalization; Copolymer

1. Introduction

Carbon fillers like carbon black, carbon nanotube, graphite or graphene are widely used for nanocomposite applications in order to improve mechanical, thermal and/or electrical properties of polymer matrices [1], [2]. The last decades, graphene and other 2D materials [3], [4] attracted much attention thanks to remarkable properties due to their 2D structure with high aspect ratio and high surface area. This exceptional structure made graphene one of the most promising particle for polymer nanocomposites elaboration. Its 2D structure mostly composed of carbon atoms with low defect concentration provides high electrical conductivity due to a solid carbon pathway for electrons [5].

However, the final performances of a nanocomposite is also affected by the dispersion of the nanoparticles in the matrix and the quality of the particle/matrix interface [6]. The strong Van der Waals interactions between π-π bonds of graphene sheets and the lack of affinity with polymer matrices entailed inevitably the aggregation of the graphene particles. That is why obtaining a percolated network in the nanocomposite is difficult and requires high content of graphene. The percolation is an essential element that corresponds to the formation of graphene sheets network and impact strongly composite electrical properties [7].

A poor interface/interphase can lead to an unbinding of the nanoparticle from the polymer matrix and have an impact on polymer and nanocomposite property [8]. To counter this phenomenon, chemical modifications of graphene as oxidation and functionalization are used to allow a better affinity with polymer matrices [9], [10]. High compatibility between graphene and the polymer matrix allows to produce performant nanocomposite. Graphene surface

modification is an effective way to improve the robustness of the polymer/particle interface. This allows charge transfer and also exploit the extraordinary properties of this carbon material [11], [12], [13]. The compatibility of graphene and polymer matrices can be improved by grafting polymer chains on graphene [14], [15]. Several methods were developed such as "grafting from", "grafting through" or "grafting onto" [16], [17], [18], [19], [20]. From this chemical modification methods, the synthesis of a conductive and compatible modified graphene with polymer matrices is possible [21], [22], [23]. The "grafting from" procedure is defined by the introduction of an initiator moiety to proceed to the grafting of polymer chains from different polymerization techniques. The "grafting through" approach is similar, but it requires the introduction of a polymerizable function during the first step. Then, a polymerization step allows the grafting of polymer chains by copolymerization with comonomers. For the "grafting onto" strategy, the polymer chains are first synthesized before to be grafted onto the graphene oxide (GO). An organic functional group from the polymer chain is generally used to form the covalent bond by condensation reaction with the reactive GO functional groups. By comparison, the "grafting onto" is a practical approach which allows the control of the polymer chain structure but the grafting density is lower compared to "grafting from" method [16], [24]. Functionalization of pristine graphene can be directly obtained [14], [25] but graphene oxide (GO) is usually selected as the starting material for the grafting of the organic groups. Indeed, reactivity of hydroxyl, carboxyl, and epoxy functions of GO allows the introduction of a large variety of chemical groups which can make carbon materials compatible with various polymer matrices. Hummers' method is the most common synthesis for graphene oxide. This method entails high defects on graphite or graphene structure and the formation of sp^3 domains due to appearance of functional groups from the oxidation reactions. This strong modification leads of a drop of the electrical property due to the sp^2 network deterioration [26], [27]. However, this chemical modification is necessary for stable dispersion, graphite exfoliation and for the formation of reactive functional sites allowing functionalization. Since graphene oxide is an electric insulator, a chemical or thermal reduction step allows the recovery of electrical properties. Hydrazine hydrate or high temperature treatments are generally used as reduction reaction [28], [29]. In this case, graphene modification with polymer chains can be associated with a good electrical conductivity for conductive nanocomposite elaboration [30]. Non-covalent functionalization is also possible by using surfactant to improve graphene dispersion in the matrix without damaging the graphene structure [31]. However, surfactants can interact with polymer matrix and alters its properties. Indeed, a high concentration of surfactant is sometimes necessary and decreases mechanical properties of the nanocomposite [32]. In this study, we will focus on chemical modification

control of graphene and graphite to adjust their electrical properties. The objective is to further promote a good graphene or graphite dispersion in a poly(methyl methacrylate) (PMMA) matrix.

In the literature, several chemical modification methods were tested on graphite and graphene [33]. However, most of the time, these chemical modifications impact on electrical property of the particles were not completely investigated. In this article, two types of oxidation treatments have been examined. The first method based on Hummers' method is a strong oxidation reaction using strong acids and oxidants. The second method is a soft oxidation procedure easier to implement and leading to less defects on the graphene sheets structure. Firstly, the objective was to characterize these two procedures and determine the impact on graphite and graphene morphology and chemical structure. Secondly, oxidized particles have been modified by adding a copolymer agent using the "grafting onto" method. The efficiency of the grafting of copolymer chains has been also compared for the two oxidation methods. Then, hydrazine hydrate reduction and thermal reduction were performed in order to recover a suitable structure for the modified graphene sheets and improve the electron transfer. In parallel to the oxidation and grafting reactions, we characterized the effect of these modifications on the electrical conductivity of the treated graphene and graphite particles.

2. Materials and methods

2.1. Raw materials

Graphene KNG 180 (Xiamen Knano), methyl methacrylate (MMA, Sigma-Aldrich), nitric acid (Sigma Aldrich), graphite (Sigma-Aldrich), sulfuric acid (Sigma Aldrich), potassium permanganate (Sigma Aldrich), Hydrogen peroxide 33% (Panreac), Hydrochloric acid 37% (Panreac), 2-hydroxyethyl methacrylate (HEMA, Sigma-Aldrich), hydrazine hydrate (Sigma-Aldrich), azobisisobutyronitrile (AIBN, Sigma-Aldrich), acetonitrile (Fisher), toluene (Fisher), acetone (Merck Schuchardt OHG) were used as received without any further purification.

2.2. Soft oxidation of graphene and graphite: Nitric acid method

Graphene and graphite were firstly oxidized (Fig. 1a) by following the procedure inspired by Zubair et al.[34]. Into a 50 mL flask equipped with a condenser, 2 g of graphene or graphite and 20 mL of concentrated nitric acid (60 wt%) were introduced. The mixture was then stirred and heated at solvent reflux for 15 h. The mixture was centrifuged at a speed of 5000 rpm to eliminate the liquid phase and then washed with deionized water until pH 5–7 was obtained.

Finally, the obtained graphene and graphite oxide was dried under vacuum before characterization. The obtained graphene and graphite oxides were named GOxN and GrOxN, respectively.

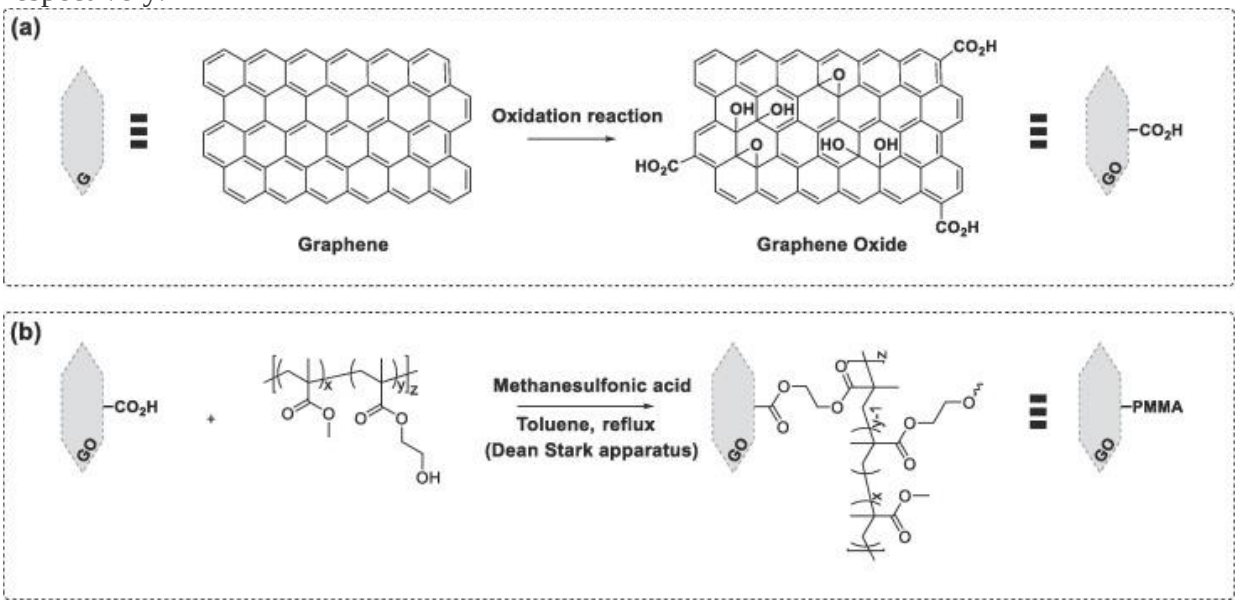

Fig. 1. Schematic representations of (a) graphene oxidation and (b) Functionalization of graphene oxide in toluene with P(MMA-co-HEMA) copolymer as grafting agent.

2.3. Strong oxidation of graphene and graphite: Hummers' method

The second method used is an improved Hummers' method [35]. This method consists in mixing 1 g of graphite or graphene with 3 g of $KMnO_4$. 45 mL of H_2SO_4 were added in order to penetrate between the sheets and to achieve the oxidation with $KMnO_4$. The solution was stirred at 40 °C during 24 h. When the oxidation was complete, the solution turned brown. 80 mL of hydrogen peroxide (33%) and deionized water (1:15) were added to the mixture. 15 mL of HCl (37%) and deionized water (1:9) were mixed with 25 mL of the graphene or graphite oxide suspension in order to remove metal ions. Finally, around 15 washes were necessary to remove acid species to reach a pH between 6 and 6.5. The obtained graphene or graphite oxide suspension was freeze-dried during 24 h in order to obtain a dry powder. The obtained graphene and graphite oxides were named GOxH and GrOxH, respectively.

2.4. Thermal and chemical reduction (r_1 and r_2)

Particles were thermally reduced at 250 °C under air during 1 h (this treatment was noted r_1). The chosen temperature rise was 3 °C/min in order to avoid deflagration phenomenon of GrOxH or GOxH [36]. The obtained reduced graphene and graphite oxides from the thermal method were named GOxH-r_1 and GrOxH-r_1, respectively.

The chemical reduction (noted r_2) of GOxH or GrOxH was also tested using hydrazine hydrate. A 3 mg/mL solution of GOxH or GrOxH in water was introduced in a flask. Then hydrazine hydrate was added at a rate of 1 µL for 3 mg of GOxH or GrOxH. The mixture was then heated at 80 °C during 12 h under stirring. The obtained solution was filtered with a fritted glass filter under vacuum [37]. The obtained reduced graphene and graphite oxide from the hydrazine method were named GOxH-r_2 and GrOxH-r_2, respectively.

2.5. Synthesis of P(MMA-co-HEMA) copolymer

The synthesis consisted in a radical copolymerization of methyl methacrylate (MMA) and 2-hydroxyethyl methacrylate (HEMA) with a molar ratio MMA/HEMA = 95/5. Into a 100 mL flask fitted with a condenser, 10 g (0.1 mol) of MMA, 0.68 g (5.2×10^{-3} mol) of HEMA, 0.16 g (9.7×10^{-4} mol) of AIBN and 20 g of acetonitrile were introduced. Argon was bubbled through the mixture for 15 min. Then the mixture was stirred and heated at 80 °C for 3 h. After reaction, the copolymer of methyl methacrylate and hydroxyethyl methacrylate P(MMA-co-HEMA) was purified by precipitation in methanol. A schematic representation of the grafting agent structure is available in Fig. 1b. SEC analysis was used to characterize the obtained copolymer, a polydispersity index of 1.47 was determined with a M_n of 35000 g.mol^{-1} equivalent PMMA. ^{1}H NMR (Figure S1) confirmed the expected structure.

2.6. Functionalization of oxidized graphene and graphite

After particles oxidation (Fig. 1a), the P(MMA-co-HEMA) copolymer was grafted to GOxH, GrOxH, GOxN and GrOxN by an esterification reaction (Fig. 1b). The esterification occurs by condensation of the hydroxyl groups of the copolymer chains with the carboxylic acid functions of the oxidized particles. 1 g of GOxN (or GrOxN, GrOxH, GOxH), 0.1 g of the P(MMA-co-HEMA) copolymer, 50 mL of toluene and 1 mg (1.04×10^{-5} mol) of methanesulfonic acid were introduced into a 50 mL flask equipped with a Dean Stark apparatus. The mixture was then stirred and heated at solvent reflux for 15 h. The Dean Stark apparatus eliminated the water formed during the reaction. The mixture was then centrifuged at a speed of 5000 rpm to eliminate the liquid phase and washed three times with acetone. The powder was dried under vacuum before characterization. The different grafted samples were listed in Table 1.

Table 1. List of the modified graphite and graphene samples, the different treatments used and the type of notation chosen.

Materials	
Gr	Graphite
G	Graphene
GrO-PMMA	Graphite oxide functionalized with P(MMA-co-HEMA)
GO-PMMA	Graphene oxide functionalized with P(MMA-co-HEMA)
Chemical, thermal treatments	
OxH	Oxidation using the Hummers' method
OxN	Oxidation using nitric acid
r_1	Thermal reduction at 250 °C
r_2	Chemical reduction using hydrazine hydrate
Modifications sequence examples	
GOxH-r_2	Hydrazine reduction of GOxH
GOxH-r_2-PMMA	Step 1: Hydrazine reduction of GOxH Step 2: functionalization with P(MMA-co-HEMA)
GOxH-PMMA-r_2	Step 1: functionalization of GOxH with P(MMA-co-HEMA) Step 2: Hydrazine reduction
GOxH-r_2-PMMA-r_1	Step 1: Hydrazine reduction on GOxH Step 2: functionalization with P(MMA-co-HEMA) Step 3: Thermal reduction at 250 °C

2.7. Characterization methods

Fourier transform infrared spectroscopy (FTIR) was used to evaluate the graphene oxidation. Analyses were conducted on a BRUKER Vertex 70 spectrometer using an attenuated total reflection (ATR) process. Spectra were obtained from 32 scans with a resolution of 4 cm^{-1} at room temperature in a wavenumber range between 4000 cm^{-1} and 400 cm^{-1}.

Thermogravimetric analysis (TGA) was carried out to evaluate the oxidation rate of graphene oxide and graphite oxide and to measure the grafting rate after modification with P(MMA-co-HEMA) copolymer. Grafting rate is determined thanks to TGA values:

$$Grafting\ rate = \frac{m_{copo\ loss}}{m_{sample}}$$

where $m_{copo\ loss}$ is the mass of copolymer grafted on graphene or graphite and msample is the powder mass analyzed by TGA.

Initial rate is determined with graphene (or graphite) and copolymer mass introduced in the reaction:

$$Initial\ rate = \frac{m_{copo}}{m_G + m_{copo}}$$

where m_{copo} and m_G are the mass of copolymer and graphene or graphite used for the reaction, respectively.

Grafting efficiency was calculated as followed:

$$Grafting\ efficiency\ (\%) = \frac{Grafting\ rate}{Initial\ rate} \times 100$$

In our synthesis conditions, molar concentration of copolymer is fixed at $2.86.10^{-6}$ mol/g of graphene or graphite.

These measurements were performed on a TGA 8000 apparatus from PERKIN ELMER under nitrogen atmosphere at a gaz flow of 40 mL/min. For each analysis the sample (5 ± 2 mg) was first maintained at 110 °C during 15 min to remove physisorbed water and then heated up to 600 °C at 10 °C/min. TGA thermograms start at 110 °C in this article.

X-ray diffraction (XRD) was used to obtain informations about the morphological changes for graphene and graphite after oxidation and functionalization. The diffractometer used is a BRUKER D8 Advance apparatus with a Cu Kα radiation (λ = 0.1542 nm). XRD technique was used to confirm the delamination and exfoliation phenomena observed for graphene after Hummer's method oxidation. XRD characterizations are based on the Bragg's law (equation (1)) to determine the interlayer distance [38], [39]:

$$d_{002} = \frac{n\lambda}{2sin\theta}$$

With d_{002} is the interlayer distance, λ is the wavelength, n is the diffraction order and θ is the diffraction angle.

The Debye Scherrer's law (equation (2)) was used to determine the graphene and graphite thicknesses [40], [41], [42]:

$$D_{002} = \frac{0.89\lambda}{FWHM\ (rad)x\ cos\theta}$$

With D_{002} corresponding to the thickness of the particle, λ to the wavelength, FWHM to the full width middle high of the peak, and θ is the diffraction angle.

Raman spectroscopy was used to analyze defects in graphene or graphite structure before and after chemical modifications. Spectra were obtained using a RENISHAW spectrometer with a confocal microsocope. Raman apparatus was used with a laser source of 532 nm.

Scanning electron microscope (SEM) micrographs were performed on an Environmental Scanning Electron Microscope equipped with Energy Dispersive X-ray spectroscopy (ESEM–EDX) (Quanta 200 FEG) from the FEI Company.

Pyrolysis–gas chromatography–mass spectrometry (Py-GC/MS) analytical setup consisted of an oven pyrolyzer connected to a GC/MS system. A pyrolyzer equipped with an electrically heating platinum filament (Pyroprobe 5000 from CDS Analytical) was used for the pyrolysis step under helium. Each sample (less than 1 mg) was introduced in a quartz tube between pieces of quartz wool. A coiled probe enabled the pyrolysis of the whole. The sample was heated directly at 900 °C (during 15 s) before gases formed during pyrolysis were drawn to the gas chromatograph (during 5 min). The pyrolyzer apparatus is connected to a gas chromatograph (450-GC from Varian) by means of a transfer line heated at 270 °C. The GC initial temperature of 70 °C was held for 0.2 min, and then raised to 310 °C at 10 °C/min. The Varian Vf-5 ms capillary column (30 m × 0.25 mm) used for separation was under helium (1 mL/min) with a split ratio set to 1:50. After separation, the pyrolysis products were introduced to the ion trap analyzer of the 240-MS mass spectrometer (Varian) through the direct-coupled capillary column. The NIST mass spectral library was used to identify the pyrolysis products.

3. Results

3.1. FTIR, TGA and Py GC/MS characterization of oxidized and functionalized graphene and graphite

The different modified samples were characterized to confirm and compare the amounts of oxidation and the exfoliation degree obtained with the two oxidation methods used.

From the Hummers' oxidation (leading to GOxH and GrOxH), several oxide groups are present on the oxidized structures as confirmed by the FTIR analysis (Fig. 2). The wide band at 3500 cm^{-1} observed for GOxH and GrOxH corresponds to –OH bonds, and signals of carbonyl and carboxyl groups are identified at 1250 cm^{-1} and 1710 cm^{-1}, respectively. The presence of the C=C bonds is confirmed by the band at 1625 cm^{-1}.

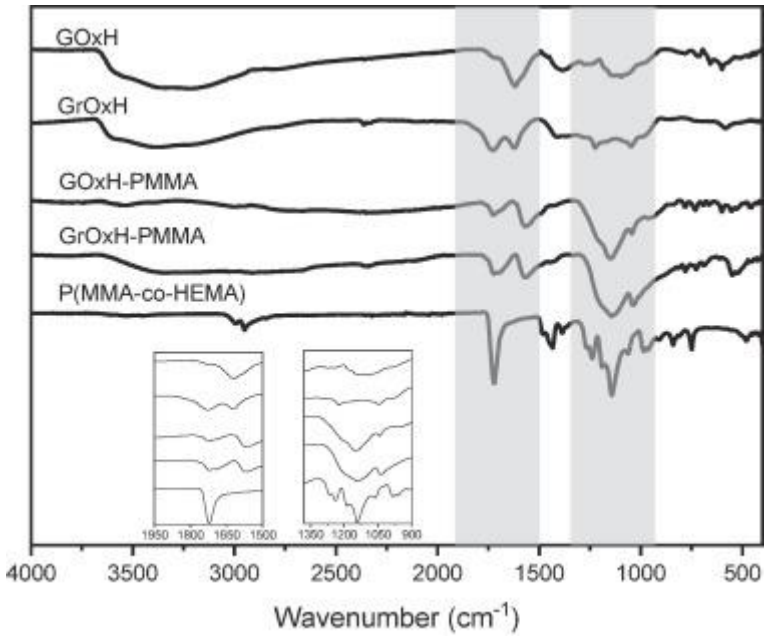

Fig. 2. FTIR of graphene and graphite samples after Hummers' oxidation and functionalization with the copolymer.

After grafting of P(MMA-co-HEMA) copolymer, the band corresponding to C-O bond at 1220 cm^{-1} is broader for GrOxH-PMMA compared to GrOxH that confirms the presence of ester groups from the copolymer. The band at 1730 cm^{-1} is characteristic of the C=O of the ester group from methacrylate units. This band proves also the copolymer presence on the graphene and graphite samples after the grafting step.

As for native graphene and graphite, GOxN and GrOxN absorb IR due to a low oxidation level. The oxidation and then the functionalization with the copolymer were not proved by the FTIR analyses for these samples.

The TGA of the oxidized particles by nitric acid shows a low oxidation rate with a percentage of residue reaching 98.9 wt% for GOxN compared to 99.1 wt% for graphene. The same result was obtained with GrOxN. However, the obtained functionalized graphene and graphite display a higher loss mass with a residue of 95.5 wt% for GOxN-PMMA and 98 wt% for GrOxN-PMMA. The grafting efficiency in our reaction conditions is 14 % and 8 % for GOxN-PMMA and GrOxN-PMMA, respectively. These results prove that a very low oxidation was obtained with nitric acid, but is enough to produce carboxyl groups on the graphene sheets to allow, by esterification, the grafting of the P(MMA-co-HEMA) copolymer chains.

TGA of the graphene and graphite oxidized by the Hummers' method display higher oxidation rates (Fig. 3a, b). A strong mass loss appears at 200 °C reaching 30 wt% corresponding to the degradation of labile oxide groups.

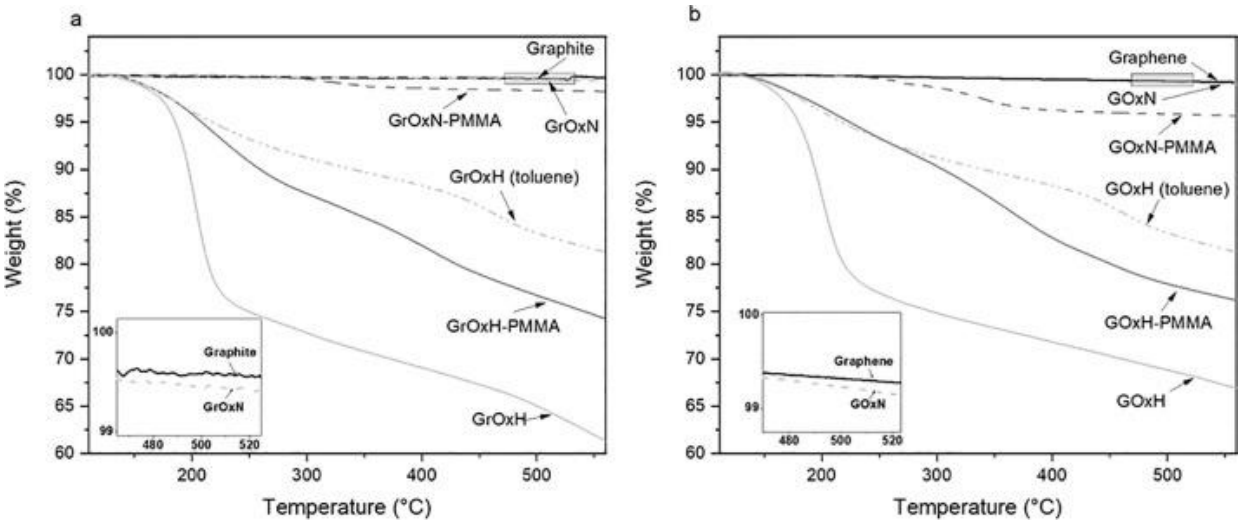

Fig. 3. TGA of (a) modified graphite and (b) modified graphene samples. GrOxH (toluene) and GOxH (toluene) were obtained from GrOxH and GOxH powders dispersed in toluene and heated at solvent reflux in the same grafting synthesis conditions than GrOxH-PMMA and GOxH-PMMA, respectively without the copolymer agent incorporation. Thermogram of P(MMA-co-HEMA) copolymer is available in Figure S2.

As for the oxidation with nitric acid, the oxidation by the Hummers' method allows the formation of carboxylic acid groups that can react with P(MMA-co-HEMA) copolymer to functionalize graphite and graphene oxide. GrOxH-PMMA displays a weak degradation at 200 °C compared to GrOxH (around 12 wt% loss and 33 wt%, respectively). The same observation is conducted for GOxH compared to GOxH-PMMA. Indeed, an in-situ reduction occurs during the synthesis due to the temperature condition at 110 °C in toluene. To verify this hypothesis the same reaction was carried out with GrOxH and GOxH without the grafting agent, GrOxH-Toluene/110 °C and GOxH-Toluene/110 °C respectively. These curves show the expected in-situ reduction during the synthesis with a lower mass loss. However, a mass loss at 450 °C, for GOxH-Toluene/110 °C and GrOxH-Toluene/110 °C, is also observed probably due to the decomposition of the trapped solvent between graphene sheets [43], [44]. Due to this trapped solvent, the copolymer grafting efficiency calculation is difficult. Indeed, trapped toluene quantity varies when this procedure is reproduced with GOxH or GrOxH.

Py-GC/MS allows to confirm the presence of the copolymer agent grafting for GOxN-PMMA, GrOxN-PMMA, GOxH-PMMA and GrOxH-PMMA samples. The chromatograms obtained for the pyrolysis of GOxN-PMMA and GrOxN-PMMA show the presence of a major peak at 3 min attributed to methyl methacrylate (MMA) (Fig. 4). For GrOxH-PMMA and GOxH-PMMA, several main peaks are observed in addition to the MMA signal during the pyrolysis, which reflects a higher degradation of the structure in comparison with GOxN-PMMA and GrOxN-PMMA. Indeed, Hummers' oxidation creates more defects than oxidation with nitric acid. These degradations can be attributed to structural weakness due to the strong oxidation

reaction of the Hummers' method, which disturbs the sp^2 structure. The MMA peak attributed to the decomposition of the grafted PMMA chains is more intense for GOxH-PMMA than GrOxH-PMMA. This result implies a higher grafting efficiency for GOxH-PMMA, this will be explained later in the study. Moreover, presence of a weight loss due to release of toluene is confirmed also with this analysis which can prove the solvent trapping between sheets.

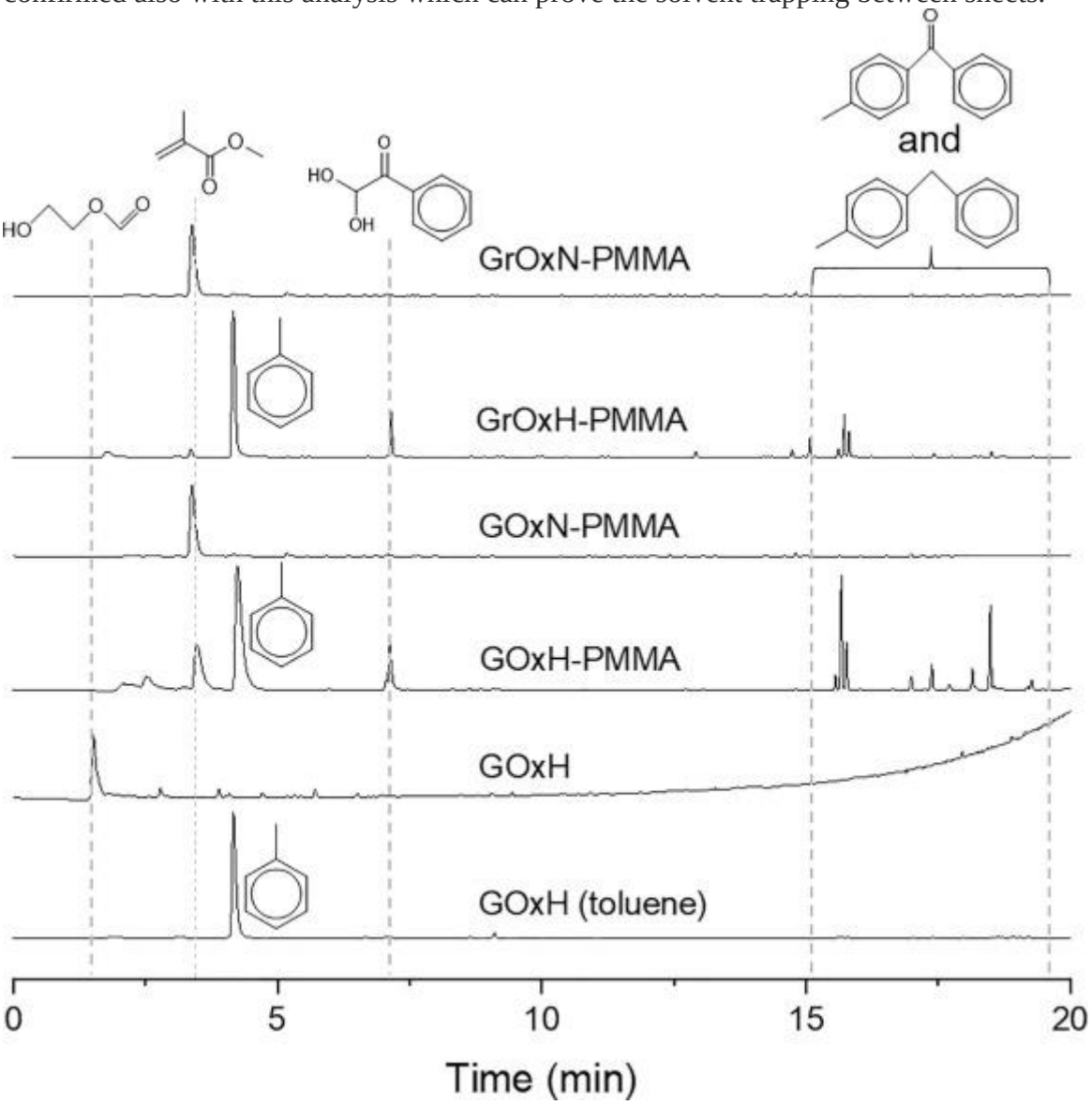

Fig. 4. Py-GC/MS chromatograms of modified graphene and graphite samples.

3.2. Morphological characterization of oxidized and functionalized graphene and graphite

After confirming oxidation and functionalization, the evolution of the morphology and the stacking structure of these materials have been studied. Information about exfoliation degree and defect concentration is essential for predicting the graphene and graphite capacity to

improve the final properties of polymer based nanocomposites, especially electrical conductivity [45].

SEM images were investigated in order to observe the impact of chemical treatments on sheets structure. Fig. 5 shows graphite and graphene particles before and after Hummers' and nitric acid oxidations. Before oxidation, Fig. 5 a and d show a compact stacking of sheets corresponding to graphite and graphene materials, respectively. After nitric acid oxidation, the morphology did not change and stay compact for oxidized graphite and graphene samples (Fig. 5 b and e, respectively). During the Hummers' oxidation, the creation of new functional groups in the intercalated position between the carbon sheets facilitate their exfoliation [46]. The SEM images of the graphite and graphene oxidized seems to prove the high exfoliation degree phenomenon (Fig. 5 c and f, respectively) with clearly more flexible and transparent sheets.

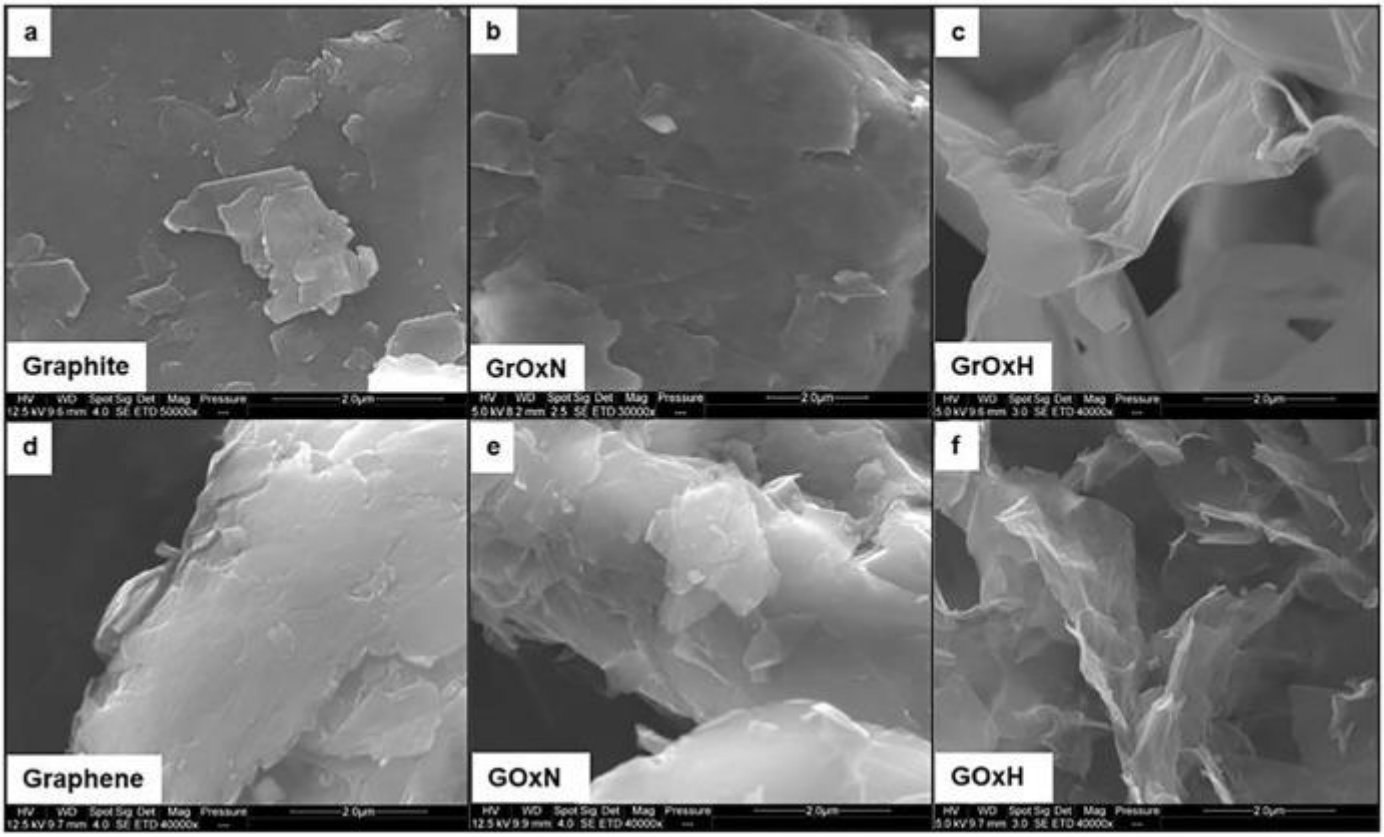

Fig. 5. SEM images of (a) graphite, (b) GrOxN, (c) GrOxH, (d) graphene, (e) GOxN and (f) GOxH.

The XRD analysis provides additional morphological information and confirm SEM observations. The typical diffractogram of graphite (Fig. 6a) shows a main peak at 26.4° corresponding to an interlayer distance of 0.337 nm and after calculation a carbon sheets stacking of 64 layers [47]. This small interlayer distance combined with strong Van der Walls interactions between sheets make the exfoliation difficult. Therefore, the use of only an ultrasonication step is not enough. Oxidation is one of the chemical ways to allow the increase of the interlayer distance. A graphene diffractogram should not show peaks due to the

monolayer structure. In this study, the used commercial graphene displays a peak at 26.4°. It assumes that this commercial graphene structure is similar as graphite with 46 layers.

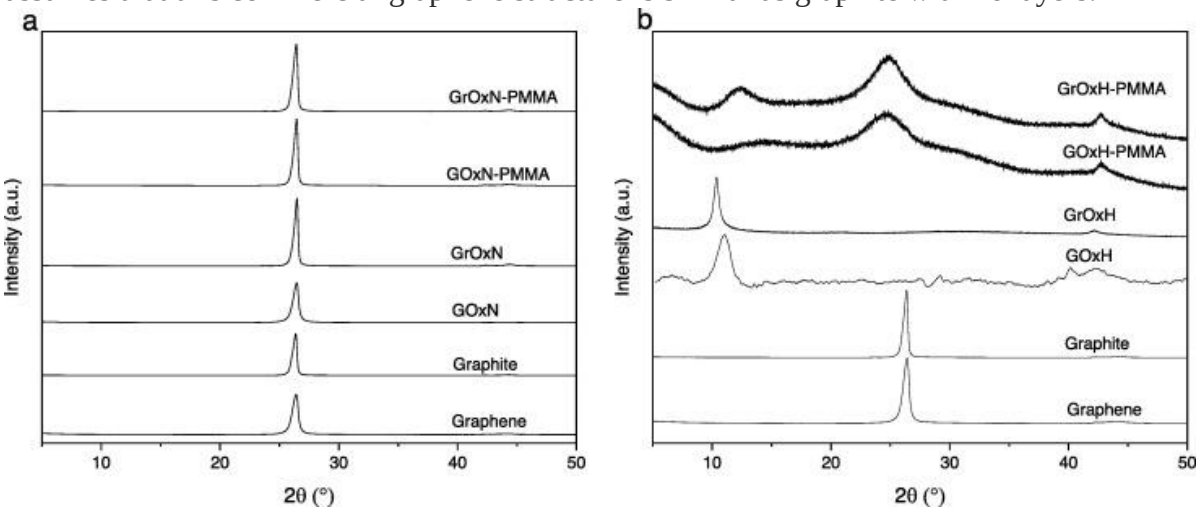

Fig. 6. XRD diffractograms of graphite and graphene samples oxidized and functionalized with P(MMA-co-HEMA) copolymer using (a) nitric acid and (b) Hummers' method.

The soft oxidation method with nitric acid is not enough to obtain intercalation of oxide groups between layers, as shown by the peak (0 0 2) at the same 2θ degree position before and after oxidation (Fig. 6a). Results are similar after functionalization for GOxN-PMMA and GrOxN-PMMA. The copolymer grafting does not change the interlayer spacing and leaves the morphology unchanged. The localization of the grafting is assumed to be only on the edge and not between graphene sheets.

On the contrary, the oxidation of graphite and graphene using the Hummers' method leads to a displacement of the (0 0 2) peak from 26.4° to 10.5° and to 11° on the XRD diffractograms, respectively (Fig. 6 b). At this 2θ position, the interlayer distance is 0.835 nm and 0.801 nm for GrOxH and GOxH, respectively due to the intercalation of oxide groups between the sheets. The interlayer distance also depends of the content of water adsorbed in the material [48]. By using Equation (2), the number of layers can be calculated and are reported in Table 2. Hummers' method displays a high exfoliation degree from 65 to 9 layers for graphite and 46 to 9 for commercial graphene, which agrees with SEM images. AFM images of GrOxH after deposition on silica wafer (Figure S3) confirmed a partial graphite exfoliation with a measured thickness of 2 and 4 nm. Same number of layers was obtained for GOxH. These results proves that GrOxH and GOxH obtained by Hummers' oxidation can be finally considered as a multilayer graphene oxide [49].

Table 2. Calculation performed from XRD diffractograms showing the impact of two different oxidation methods on graphite and graphene interlayer distance and thickness.

Materials	Peak position (°)	Interlayer spacing (nm)	FWHM (rad)	Particle thickness (nm)	Layers number
Graphite	26.42	0.337	0.0066	21.33	63–64
GrOxH	10.58	0.835	0.0174	7.91	9–10
GrOxN	26.42	0.337	0.0064	21.99	65–66
Graphene	26.42	0.337	0.0090	15.64	46–47
GOxH	11.03	0.801	0.0188	7.32	9–10
GOxN	26.42	0.337	0.0094	14.97	44–45

XRD patterns of GOxH-PMMA and GrOxH-PMMA are plotted in Fig. 6b. After functionalization, the peak at 10.4° shifts to 24.9° for both GrOxH-PMMA and GOxH-PMMA which indicates that the interlayer distance decreases from 0.835 and 0.801 nm, respectively to 0.357 nm. This shift is assigned to a partial restacking after the functionalization. Indeed, functionalization is performed at 110 °C and reduction of labile groups can occur at this temperature. Figure S4 proves that by putting GOxH in toluene at 110 °C it is possible to decrease the interlayer spacing by reduction of oxygenated groups. As the grafting of P(MMA-co-HEMA) copolymer occurs at the edge of the graphene sheets and not in the internal structure it does not allow to increase the interlayer spacing. In the case of grafting in the internal structure, the interlayer can increase [23], [50]. The broad peak at 12° for GrOxH-PMMA (and less pronounced for GOxH-PMMA) can be assigned to the presence of the oxygenated groups in some part of the graphene particles that were not fully reduced.

Since electrical conductivity depends on the graphene structure such as the defect concentration, Raman spectroscopy was used to evaluate the concentration of defects in the graphene and graphite sheets structure of the chemically modified samples [51]. For pristine graphite or graphene, two bands appear at 1351 cm^{-1} and 1581 cm^{-1}, corresponding to the D and G bands, respectively. The G band corresponds to the E_{2g} optical phonon whereas the D band corresponds to the A_{1g} optical phonon [52]. The comparison of D and G band intensities (I_D/I_G ratio) of particles modified from nitric acid method shows that the structure of graphene is preserved even after oxidation and functionalization (Fig. 7 a). On the other hand, oxidation by Hummers method leads to a strong degradation of the graphene and graphite structure due to the introduction of sp^3 clusters confirmed with a higher I_D/I_G ratio (Fig. 7 b). For samples GOxH and GrOxH, the value is closed to 1 which reveals the presence of high concentration of defects or disorders in the sheets structure. After functionalization, the I_D/I_G ratio increases strongly for GOxH-PMMA compared to GrOxH-PMMA. This increase in defects has been attributed to a higher grafting efficiency of the copolymer grafting agent for GOxH-PMMA.

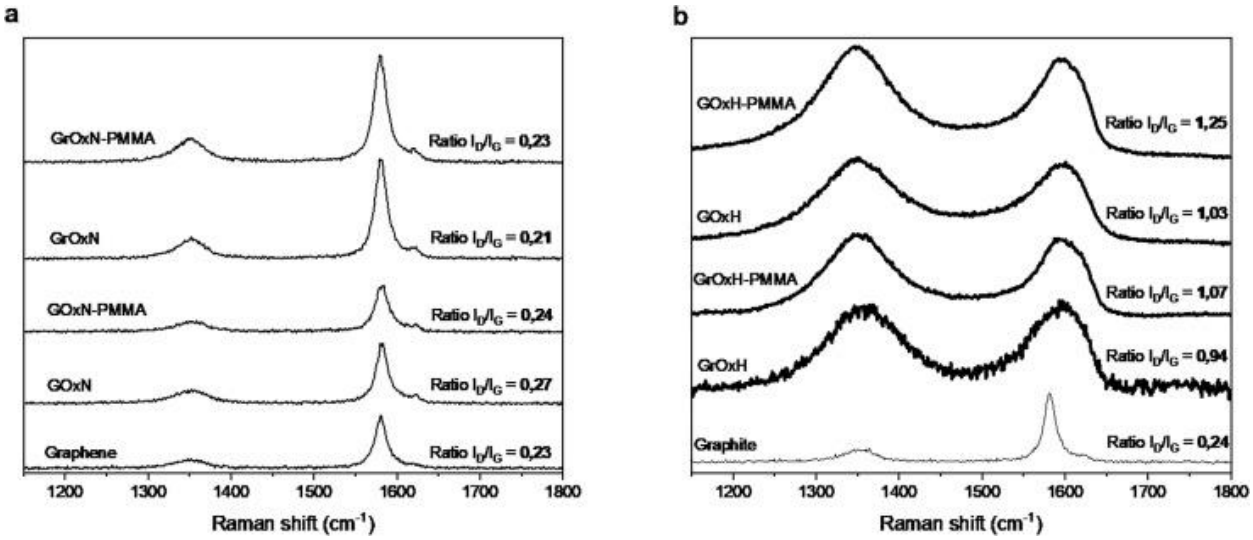

Fig. 7. Raman spectra of graphene and graphite before and after modifications from (a) nitric acid and (b) Hummers' methods.

3.3. Thermal and chemical reduction of oxidized and functionalized graphene and graphite

3.3.1. Reduction of graphite and graphene oxide

Reduction of graphene or graphite oxide obtained from Hummers' method is necessary to recover a sp^2 structure and good electrical properties. The reduction method can be a chemical or a thermal treatment [53], [54]. By comparing hydrazine reduction and thermal reduction, mass losses occur at different temperatures when samples are analyzed by TGA. We assume that hydrazine reduction and thermal reduction decompose different oxygenated groups. Indeed, the thermograms comparison shows different degradation profiles.

Fig. 8 shows the effective thermal and chemical reduction of Hummers' oxidized graphene and graphite. Indeed, the absence of weight loss at 200 °C for GrOxH-r_1 and GrOxH-r_2 compared to GrOxH and GOxH proves the effectiveness of the reductions.

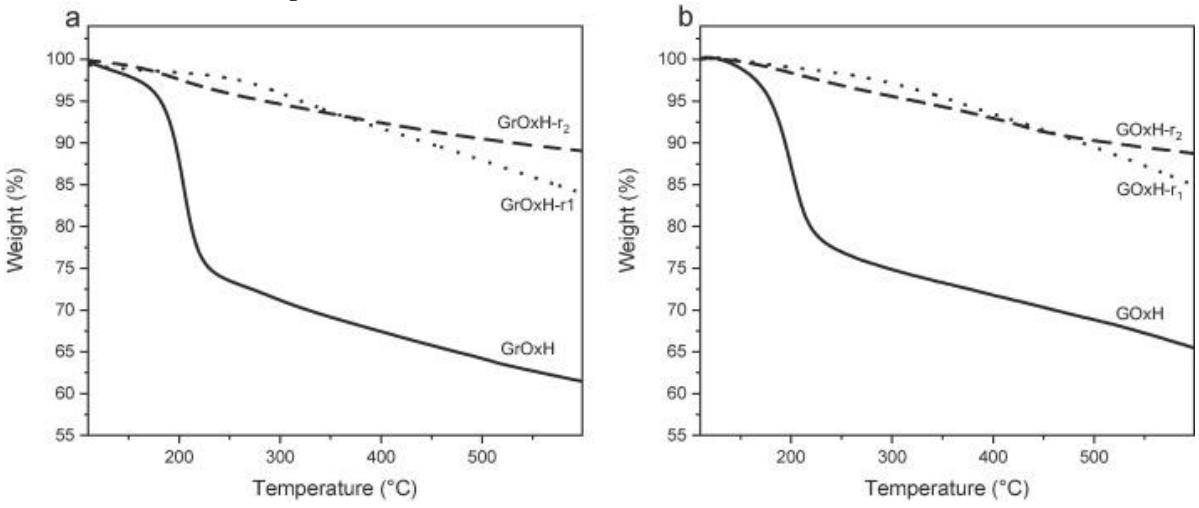

Fig. 8. TGA of (a) GrOxH-r_1 (thermal reduction), GrOxH-r_2 (chemical reduction) and GrOxH, and (b) GOxH-r_1, GOxH-r_2 and GOxH.

After reduction, the elimination of the intercalated oxygenated groups leads to a restacking of the carbon sheets as shown by XRD (Fig. 9a) with a displacement of the peak from 10.5° to 24° for both GrOxH-r_2 and GrOxH-r_1. This latter displacement corresponds to an interlayer spacing of 0.376 nm close to the graphite structure and confirms a restacking due to oxygenated groups decomposition. The broad peak of the graphite oxide particles reduced by the thermal treatment (GrOxH-r_1) means that a low thickness of the particle is preserved after reduction with also a low number of layers. The combination of the (0 0 2) peak enlargement and the shift at 24° corresponds to particles of around 8 layers determined with Scherrer's equation. It proves that the number of layers remains the same after the reduction of GrOxH. The same restacking phenomenon (Fig. 9a) is observed with the GrOxH reduced with hydrazine hydrate (GrOxH-r_2) which can prove indirectly, the elimination of the intercalated oxygenated groups [55]. SEM images confirms the flexibility and the high degree of exfoliation with clear wrinkled and transparent particles (Fig. 9b, c).

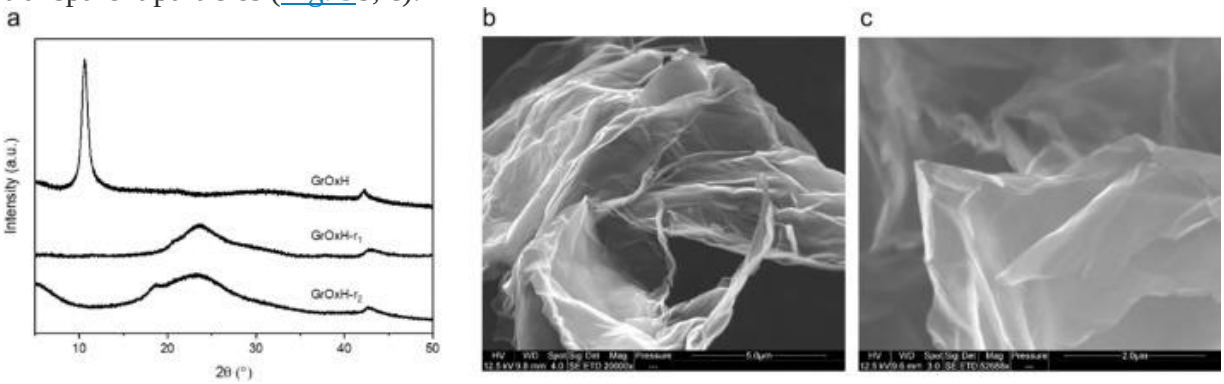

Fig. 9. (a) XRD diffractograms of reduced GrOxH by hydrazine hydrate (GrOxH-r_2) and thermal treatment (GrOxH-r_1). SEM images of (b) GrOxH-r_1 and (c) GrOxH-r_2.

3.3.2. Reduction of functionalized graphite and graphene

3.3.2.1. Reduction after the functionalization

GrOxH-PMMA and GOxH-PMMA were thermally reduced at 250 °C (leading to GrOxH-PMMA-r_1 and GOxH-PMMA-r_1) in order to decompose functional groups that disrupt sp^2 structure and which do not participate to the reaction with the grafting agent. A clear mass loss gap is observed between GrOxH-r_1 and GrOxH-PMMA-r_1 which proves the grafting agent stability during the thermal reduction (Fig. 10a). An identical phenomenon is obtained with the hydrazine hydrate reduction (GrOxH-PMMA-r_2 and GOxH-PMMA-r_2) which confirms also the stability of the grafted copolymer. Py-GC/MS also proves the presence of the copolymer grafting after the hydrazine hydrate reduction with the characteristic peak of the methyl

methacrylate (peak number 1 in Fig. 10b). Molecules containing nitrogen atoms are also released during the pyrolysis step of the reduced samples. Indeed, during the reduction, hydrazine hydrate reacts with GO and can also form nitrogen-carbon bonds.

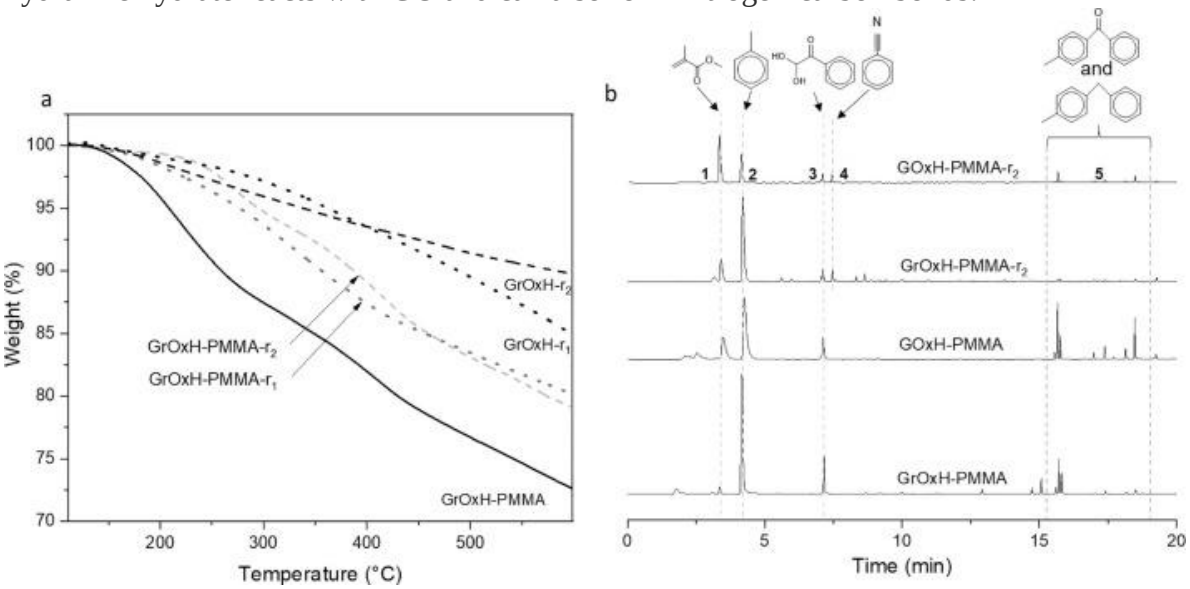

Fig. 10. (a) TGA and (b) Py-GC/MS after reduction treatment of functionalized graphite and graphene.

3.3.2.2. Reduction treatment before the functionalization

Another chemical sequence modification has been tested to evaluate the impact of the reduction treatments on the functionalization efficiency and also on the electrical conductivity. It is known that hydrazine hydrate reacts mostly with the epoxy groups and maintain the majority of carboxylic acid groups on graphite and graphene oxide [56]. So, the chemical reduction of GrOxH and GOxH can be performed before the functionalization with the copolymer grafting agent. TGA (Fig. 11a) shows that the copolymer grafting after the hydrazine reduction (GOxH-r_2-PMMA) is effective due to a higher mass loss of GOxH-r_2-PMMA compared to GOxH-r_2. Moreover, a thermal treatment after this procedure (hydrazine reduction followed by copolymer functionalization) removed other functional groups, which was not used for the copolymer grafting. Indeed, the sample obtained after this third step (GOxH-r_2-PMMA-r_1) did not highlight a mass loss at 200 °C contrary to GOxH-r_2-PMMA. Moreover, the functionalized particles (GOxH-r_2-PMMA and GOxH-r_2-PMMA-r_1) have a similar mass loss of 15 wt% between 250 °C and 400 °C corresponding to the decomposition of grafted copolymer chains. This proves that the grafted copolymer was not affected by the following thermal treatment at 250 °C. Considering the proportion of the grafting agent and graphene used during the functionalization reaction, the grafting efficiency in our reaction conditions is still 100 % after the hydrazine reduction. This result confirms also that all the copolymer chains incorporated during the reaction were fully grafted on GOxH-r_2 which is due to a high concentration of acid

carboxylic groups even after hydrazine reduction. The presence of the copolymer after the grafting reaction was proved also by Py-GC/MS (Fig. 11b). Py-GC/MS reveals numerous peaks but the identification of the copolymer is confirmed by the presence of methyl methacrylate (peak number 4 in Fig. 11b). Presence of molecules containing nitrogen atoms (peak 2 and 6 of Fig. 11b) is also observed. This was attributed to the formation of functional groups containing nitrogen atoms by the reaction of hydrazine hydrate with GOxH and GrOxH during the reduction reaction. Several other peaks appear on the chromatogram due to the different chemical treatments which lead to the creation of defects.

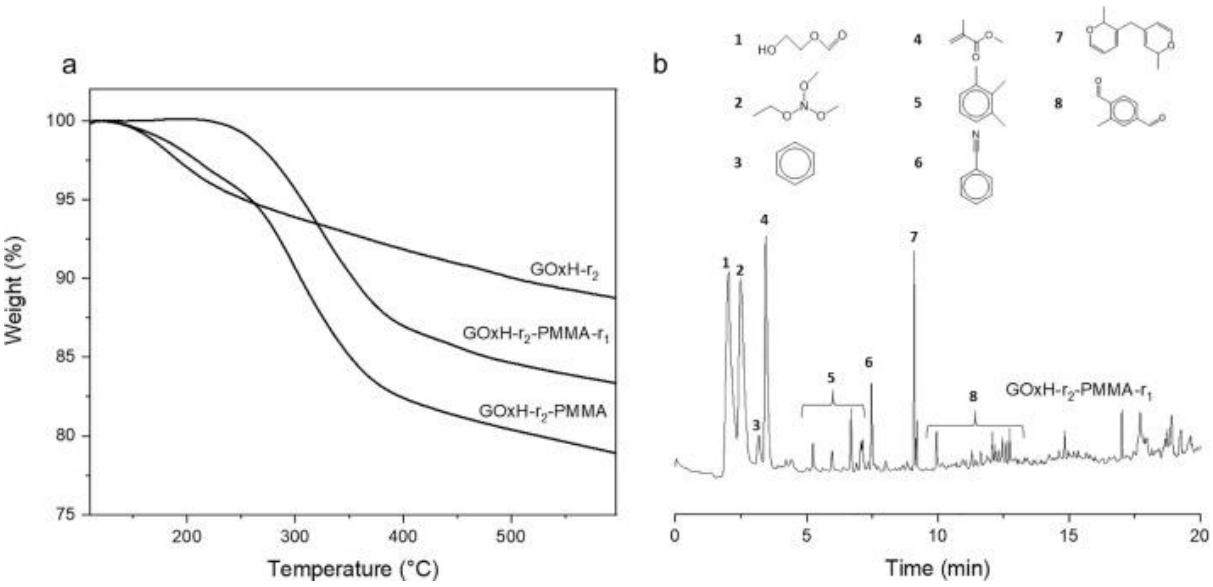

Fig. 11. (a) TGA of oxidized graphene after hydrazine reduction, copolymer grafting and thermal treatment; (b) Py-GC/MS of GOxH-r_2-PMMA-r_1.

3.4. Electrical conductivity measurement on oxidized and functionalized graphite and graphene

In the perspective to produce electrically conductive nanocomposites, electrical tests were carried out on these various samples directly on the powders (Figure S5). Four samples were prepared for each powder in order to check the reproducibility of the method. As it was demonstrated previously, the different samples tested have different chemical structure and morphology. To measure their electrical resistance, a tape with two adhesive faces was placed on a glass and then each powder sample was spread on the other surface (as presented in the scheme in Figure S5). The dimension of the tape and the power mass was identical for each sample. The objective is to measure the impact of the different chemical modifications on the electrical properties. A diode was added to the electrical circuit to confirm the conductive property of the powder. The four probes installation was elaborated to determine the resistance of the powder. A green color presented in Table 3 corresponds to the lit diode (Figure S5).

Chemical reactions on graphite and graphene obviously disturbed the sp^2 carbon structure and led to a drop of the electrical conductivity. However, these modifications are often necessary before the incorporation of graphite and graphene in polymer matrices to improve the particle dispersion and the particle/polymer interface quality. Pristine materials display very low resistance, 49.8 ± 0.4 Ω for G and 114 ± 3 Ω for Gr. Modifications from Hummers' method showed high destruction of the graphene and graphite structure. These results are confirmed by the electrical measurements in which no current is detected (Figure 12a). On the contrary, chemical modifications with nitric acid method displayed lower defects and a preservation of most of the structure. Indeed, slightly higher resistances are obtained compared to pristine materials with 100 ± 3 Ω for GOxN and 169 ± 5 Ω for GrOxN. After functionalization with the P(MMA-co-HEMA) copolymer, resistances increase inevitably. Resistances of 2566 ± 85 Ω and 57762 ± 1681 Ω are reached for GOxN-PMMA and GrOxN-PMMA, respectively (Figure 12b). For GrOxN-PMMA, the resistance increases strongly while GOxN-PMMA maintains a low resistance. This phenomenon can be due to a lower specific surface area of graphite than graphene. Specific surface areas of 2.91 m^2/g and 22.17 m^2/g were obtained by BET analyses of graphite and graphene, respectively. The low specific surface area combined with the copolymer grafting, hinders electrons displacements [57].

Table 3. Powder sample resistance values.

Materials	Resistance (Ω)	Diode (On/Off)
Graphite	114 ± 3	
Graphene	49.8 ± 0.4	
GrOxN	169 ± 5	
GOxN	100 ± 3	
GrOxH	No signal	
GOxH	No signal	
GrOxN-PMMA	57762 ± 1681	
GOxN-PMMA	2566 ± 85	
GrOxH-PMMA	No signal	
GOxH-PMMA	No signal	
GrOxH-r_1	550030 ± 9594	
GOxH-r_1	164880 ± 3368	
GrOxH-r_2	47622 ± 1066	
GOxH-r_2	1067 ± 54	
GrOxH-PMMA-r_1	No signal	
GOxH-PMMA-r_1	252041 ± 7753	
GrOxH-PMMA-r_2	No signal	
GOxH-PMMA-r_2	55585 ± 6957	
GrOxH-r_2-PMMA	409058 ± 8900	
GOxH-r_2-PMMA	6113 ± 96	
GrOxH-r_2-PMMA- r_1	232684 ± 2998	
GOxH-r_2-PMMA- r_1	4576 ± 64	
GrOxH-r_2-PMMA- r_1 (6h)	122652 ± 1505	
GOxH-r_2-PMMA- r_1 (6h)	1203 ± 3	

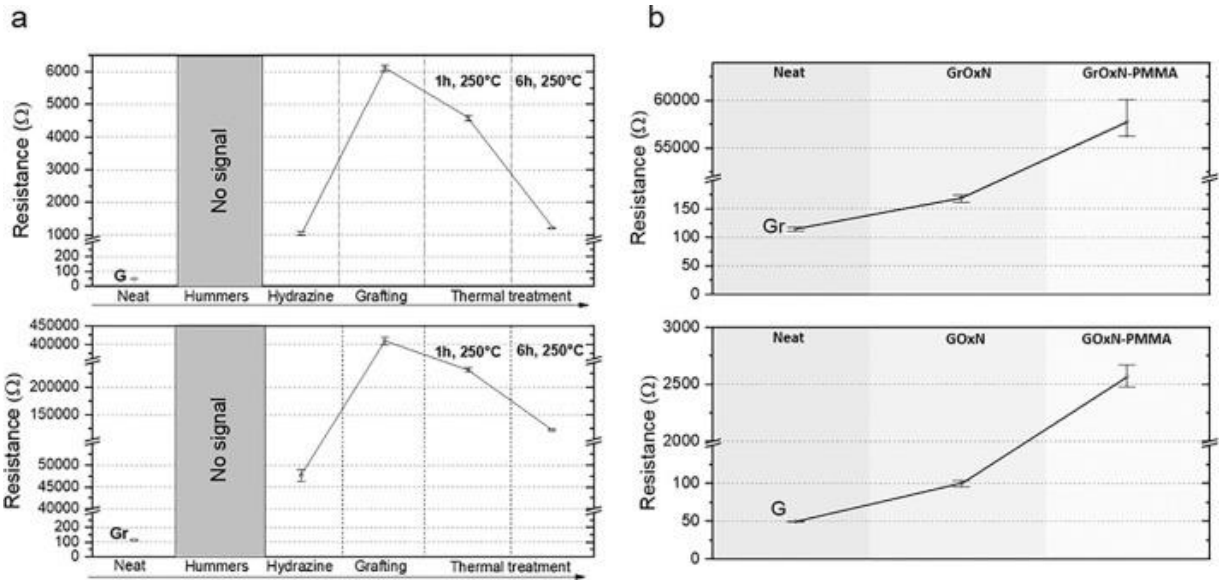

Fig. 12. (a) Impact of Hummers' method and following chemical modifications on graphene and graphite electrical property, (b) Impact of nitric acid sequence on graphene and graphite electrical property.

The thermal reduction at 250 °C allows to reduce the resistance but it needs higher temperature under control atmosphere to improve the decomposition of all oxygenated groups. Hydrazine reduction method allows to strongly decrease the resistance for GOxH-r_2 and GrOxH-r_2 which reaches $1067 \pm 54\ \Omega$ and $47622 \pm 1066\ \Omega$, respectively. The hydrazine hydrate reduction method decomposed most of the epoxide groups in the sp^3 structure and allows to recover better electrical property. However, the same reduction on functionalized particles (GOxH-PMMA-r_2 and GrOxH-PMMA-r_2) does not allow to obtain better electrical properties due to the presence of a large quantity of copolymer grafted. The presence of the grafted copolymer chains is supposed to prevent the access of hydrazine hydrate, because of steric hindrance, to the graphene structure and also to the oxygenated groups. Thermal reduction at 250 °C is more efficient to reduce the resistance in the presence of the copolymer grafting.

By changing the chemical modification sequences, the particle structure is modified and electrical properties are different. A first reduction by hydrazine of GrOxH or GOxH (GrOxH-r_2, GOxH-r_2), decomposed preferably epoxide groups while keeping carboxylic acid groups which can react by esterification with the copolymer grafting agent [58]. After the functionalization, resistance increases until $6113 \pm 97\ \Omega$ for GOxH-r_2-PMMA and until $409058 \pm 8900\ \Omega$ for GrOxH-r_2-PMMA (Figure 12a). By adding a thermal reduction step, measured resistances decrease until $4576 \pm 64\ \Omega$ for GOxH-r_2-PMMA-r_1 and $232684 \pm 2998\ \Omega$ for GrOxH-r_2-PMMA-r_1. With an extension of thermal reduction time until 6 h at 250 °C, resistance of GOxH-r_2-PMMA-r_1 (6 h) reaches $1203 \pm 3\ \Omega$ and $122652 \pm 1505\ \Omega$ for GrOxH-r_2-PMMA-$r_{1\ (6\ h)}$. The final step with the thermal reduction allows to decompose the oxygenated groups which didn't participate to the functionalization. The elimination of these residual groups improves even more the electrical conductivity. This part proved that the control of each chemical modification step and also the sequence of these steps have an impact on the material electrical properties. According to the needs and the targeted applications, electrical property can so be adjusted.

4. Discussion

Regarding electrical resistance values, hydrazine reduction before functionalization is the suitable way to obtain an exfoliated modified and conductive graphene. Hydrazine allows to recover electrical property thanks to the decomposition of a high quantity of oxygenated groups localized in the internal structure such as epoxide and open ways for electrons

circulation. Raman spectra (Figure S6 and Table S1) confirms the diminution of oxygenated groups with a FWHM reduction of D band and G band after hydrazine treatment compared to GOxH. A high D band intensity of GOxH-r_2 can be explained by the presence of vacancy defects after the subsequent chemical modifications (strong oxidation and reduction) [59]. The presence of vacancy defects does not allow to recover the electrical conductivity of the started material (graphene or graphite), but they seem to have a lower impact on electrical conductivity compared to the oxidation which create sp^3 domains in the structure. Electrons can find a pathway between vacancy defects. The functionalization on GOxH-r_2 (GOxH-r_2-PMMA) does not result in an augmentation of the FWHM. However, the I_D/I_G ratio increases after the grafting due to the presence of the copolymer mainly on the edge and not in the internal structure, since the D band is sensitive to edge defects [60]. Consequently, the presence of the copolymer increases the electrical conductivity. Hydrazine reduction after the functionalization (GOxH-PMMA-r_2) is less effective than before the copolymer grafting (GOxH-r_2-PMMA) due to the steric hindrance of the grafted copolymer which prevents hydrazine hydrate access to the internal structure.
By modifying graphene with the soft chemical sequence (OxN), reduction steps were not necessary to obtain an electrically conductive and modified graphene. However, in this way, particles are not exfoliated.

With graphite as the starting material, electrical resistances were higher compared to commercial graphene for each chemical modifications. Specific surface area is probably the parameter that influences this gap of electrical conductivity.

5. Conclusion

This study showed that for graphene and graphite it was possible to control the particles morphology and structure and therefore their electrical properties by the aid of different chemical methods and treatments. A strong oxidation treatment by Hummers' method allowed to obtain exfoliated graphene and graphite with a highly reduced numbers of layers and an increased interlayer spacing (between 9 and 10 and around 0.3 nm, respectively for both GrOxH and GOxH). Using nitric acid, oxidation allowed to create reactive site for the functionalization but the product was not exfoliated and both GrOxN and GOxN keep their original structures.
The functionalization of graphene and graphite was done using a simple and versatile "grafting onto" method which allowed the grafting of a suitable copolymer via an esterification reaction. As expected, grafting of P(MMA-co-HEMA) copolymer on both GrOxN and GOxN leads to highly conductive particles but with low amounts of grafted PMMA chains. On the contrary,

the oxidation by Hummer's method was much more efficient to create reactive sites. Moreover, by using Hummers' method graphite can be used as a less expensive and more available product than graphene. Copolymer grafting on GrOxH and GOxH are very efficient but leads to very high resistance. Hence, those nanoparticles need a reduction step to recover their electrical conductivity.
Electrical results obtained were in accordance with the physical and chemical characterizations carried out on all the nanoparticles. Resistance measurements showed that it is possible to adjust nanoparticles property of our started material via different chemical modifications such as functionalization, oxidation, thermal and chemical reduction.

These results demonstrate the possibility to combine high electrical property and graphene covalent bonding modification to further improve dispersion in polymer matrix in the perspective of the high nanocomposite performance elaboration. To complete this work, a next study will be focus also on the impact of these modifications on nanoparticles localization in an immiscible PMMA/PS blend. This will assess to evaluate the effect of these different treatments on the electrical conductivity of the obtained composite materials. One objective will be to selectively disperse those functionalized graphene or graphite into a PS/PMMA blend to try to reach a double percolation phenomenon. We assume that the most interesting modified nanoparticles that would be selectively dispersed in a PMMA/PS polymer blends would be GOxH-r_2-PMMA, GOxH-r_2-PMMA-r_1, GOxN-PMMA, GOxN and GOxH-r_2 because of their high electrical conductivity and also their different morphology.

CRediT authorship contribution statement

Thibaut Lalire: Formal analysis, Methodology, Investigation, Writing – original draft. **Claire Longuet:** Writing – review & editing, Supervision. **Aurélie Taguet:** Writing – review & editing, Supervision. **Belkacem Otazaghine:** Conceptualization, Writing – review & editing.

Acknowledgements

We gratefully acknowledge Thierry MICHEL (Laboratoire Charles Coulomb, UMR 5221 CNRS, Univ Montpellier) for Raman spectroscopy analyzes, Jean-Claude ROUX (C2MA, PCH, IMT Mines Alès) for SEM images and Monica PUCCI (LMGC, IMT Mines Ales, Univ Montpellier) for AFM images. Ecole Doctorale Sciences Chimiques Balard (Univ Montpellier) finances this work.

References

[1] D.G. Papageorgiou, I.A. Kinloch, R.J. Young, Mechanical properties of graphene and graphene-based nanocomposites, Progress in Materials Science. 90 (2017) 75–127. https://doi.org/10.1016/j.pmatsci.2017.07.004.

[2] A.A. Balandin, S. Ghosh, W. Bao, I. Calizo, D. Teweldebrhan, F. Miao, C.N. Lau, Superior thermal conductivity of single-layer graphene, Nano Letters. 8 (2008) 902–907. https://doi.org/10.1021/nl0731872.

[3] B. Li, P. Gu, Y. Feng, G. Zhang, K. Huang, H. Xue, H. Pang, Ultrathin Nickel–Cobalt Phosphate 2D Nanosheets for Electrochemical Energy Storage under Aqueous/Solid-State Electrolyte, Advanced Functional Materials. 27 (2017). https://doi.org/10.1002/adfm.201605784.

[4] B. Liu, K. Zhou, Recent progress on graphene-analogous 2D nanomaterials: Properties, modeling and applications, Progress in Materials Science. 100 (2019) 99–169. https://doi.org/10.1016/j.pmatsci.2018.09.004.

[5] Y. Zhu, S. Murali, W. Cai, X. Li, J.W. Suk, J.R. Potts, R.S. Ruoff, Graphene and graphene oxide: Synthesis, properties, and applications, Advanced Materials. 22 (2010) 3906–3924. https://doi.org/10.1002/adma.201001068.

[6] J. Wang, X. Jin, C. Li, W. Wang, H. Wu, S. Guo, Graphene and graphene derivatives toughening polymers: Toward high toughness and strength, Chemical Engineering Journal. 370 (2019) 831–854. https://doi.org/10.1016/j.cej.2019.03.229.

[7] C.W. Nan, Y. Shen, J. Ma, Physical properties of composites near percolation, Annual Review of Materials Research. 40 (2010) 131–151. https://doi.org/10.1146/annurev-matsci-070909-104529.

[8] S. Fu, Z. Sun, P. Huang, Y. Li, N. Hu, Some basic aspects of polymer nanocomposites: A critical review, Nano Materials Science. 1 (2019) 2–30. https://doi.org/10.1016/j.nanoms.2019.02.006.

[9] D. Ege, A.R. Kamali, A.R. Boccaccini, Graphene Oxide/Polymer-Based Biomaterials, Advanced Engineering Materials. 19 (2017) 16–34. https://doi.org/10.1002/adem.201700627.

[10] Y.J. Wan, L.C. Tang, D. Yan, L. Zhao, Y.B. Li, L. Bin Wu, J.X. Jiang, G.Q. Lai, Improved dispersion and interface in the graphene/epoxy composites via a facile surfactant-assisted process, Composites Science and Technology. 82 (2013) 60–68. https://doi.org/10.1016/j.compscitech.2013.04.009.

[11] V.B. Mohan, K. Lau, D. Hui, D. Bhattacharyya, Graphene-based materials and their composites: A review on production, applications and product limitations, Composites Part B: Engineering. 142 (2018) 200–220. https://doi.org/10.1016/j.compositesb.2018.01.013.

[12] J. Ma, Q. Meng, A. Michelmore, N. Kawashima, I. Zaman, C. Bengtsson, H.C. Kuan, Covalently bonded interfaces for polymer/graphene composites, Journal of Materials Chemistry A. 1 (2013) 4255–4264. https://doi.org/10.1039/c3ta01277h.

[13] A.S. Zainal Abidin, K. Yusoh, S.S. Jamari, A.H. Abdullah, Z. Ismail, Surface functionalization of graphene oxide with octadecylamine for improved thermal and mechanical properties in polybutylene succinate nanocomposite, Polymer Bulletin. 75 (2018) 3499–3522. https://doi.org/10.1007/s00289-017-2217-6.

[14] G. Yang, D. Bao, H. Liu, D. Zhang, N. Wang, H. Li, Functionalization of Graphene and Applications of the Derivatives, Journal of Inorganic and Organometallic Polymers and Materials. 27 (2017) 1129–1141. https://doi.org/10.1007/s10904-017-0597-6.

[15] Z. Tang, H. Kang, Z. Shen, B. Guo, L. Zhang, D. Jia, Grafting of polyester onto graphene for electrically and thermally conductive composites, Macromolecules. 45 (2012) 3444–3451. https://doi.org/10.1021/ma300450t.

[16] J. Liu, Y. Ye, Y. Xue, X. Xie, Y.W. Mai, Recent advances in covalent functionalization of carbon nanomaterials with polymers: Strategies and perspectives, Journal of Polymer Science, Part A: Polymer Chemistry. 55 (2017) 622–631. https://doi.org/10.1002/pola.28426.

[17] Z. Sekhavat Pour, M. Ghaemy, Polymer grafted graphene oxide: For improved dispersion in epoxy resin and enhancement of mechanical properties of nanocomposite, Composites Science and Technology. 136 (2016) 145–157. https://doi.org/10.1016/j.compscitech.2016.10.014.

[18] P. Eskandari, Z. Abousalman-Rezvani, H. Roghani-Mamaqani, M. Salami-Kalajahi, H. Mardani, Polymer grafting on graphene layers by controlled radical polymerization, Advances in Colloid and Interface Science. 273 (2019) 102021. https://doi.org/10.1016/j.cis.2019.102021.

[19] C. Han, Y.H. Li, M.Y. Qi, F. Zhang, Z.R. Tang, Y.J. Xu, Surface/Interface Engineering of Carbon-Based Materials for Constructing Multidimensional Functional Hybrids, Solar RRL. 4 (2020) 1900577. https://doi.org/10.1002/solr.201900577.

[20] Q. Quan, X. Lin, N. Zhang, Y.J. Xu, Graphene and its derivatives as versatile templates for materials synthesis and functional applications, Nanoscale. 9 (2017) 2398–2416. https://doi.org/10.1039/c6nr09439b.

[21] R.V. Héctor Aguilar-Bolados, Mehrdad Yazdani-Pedram, Eduardo Quinteros-Jara, Quimberly

Cuenca-Bracamonte, Raúl Quijada, Javier Carretero-González, Francis Avilés, Miguel A. Lopez-Manchado, Synthesis of sustainable, lightweight and electrically conductive polymer brushes grafted multi-layer graphene oxide, Polymer Testing. (2020) 106986. https://doi.org/10.1016/j.polymertesting.2020.106986.

[22] S. Park, S. He, J. Wang, A. Stein, C.W. Macosko, Graphene-polyethylene nanocomposites: Effect of graphene functionalization, Polymer. 104 (2016) 1–9. https://doi.org/10.1016/j.polymer.2016.09.058.

[23] A. Guimont, E. Beyou, P. Cassagnau, G. Martin, P. Sonntag, F. D'Agosto, C. Boisson, Grafting of polyethylene onto graphite oxide sheets: A comparison of two routes, Polymer Chemistry. 4 (2013) 2828–2836. https://doi.org/10.1039/c3py00160a.

[24] N. Rubio, H. Au, H.S. Leese, S. Hu, A.J. Clancy, M.S.P. Shaffer, Grafting from versus Grafting to Approaches for the Functionalization of Graphene Nanoplatelets with Poly(methyl methacrylate), Macromolecules. 50 (2017) 7070–7079. https://doi.org/10.1021/acs.macromol.7b01047.

[25] J. Park, M. Yan, Covalent Functionalization of Graphene with Reactive Intermediates, Accounts of Chemical Research. 46 (2013) 181–189. https://doi.org/10.1021/ar300172h.

[26] P. Feicht, S. Eigler, Defects in Graphene Oxide as Structural Motifs, ChemNanoMat. 4 (2018) 244–252. https://doi.org/10.1002/cnma.201700357.

[27] J. Park, Y.S. Kim, S.J. Sung, T. Kim, C.R. Park, Highly dispersible edge-selectively oxidized graphene with improved electrical performance, Nanoscale. 9 (2017) 1699–1708. https://doi.org/10.1039/c6nr05902c.

[28] P. Zhu, M. Shen, S. Xiao, D. Zhang, Experimental study on the reducibility of graphene oxide by hydrazine hydrate, Physica B: Condensed Matter. 406 (2011) 498–502. https://doi.org/10.1016/j.physb.2010.11.022.

[29] S.H. Huh, Thermal Reduction of Graphene Oxide, in: Physics and Applications of Graphene - Experiments, 2011: pp. 73–90. http://www.intechopen.com/books/physics-and-applications-of-graphene-experiments/thermal-reduction-of- graphene-oxide.

[30] Y. Tan, L. Fang, J. Xiao, Y. Song, Q. Zheng, Grafting of copolymers onto graphene by miniemulsion polymerization for conductive polymer composites: Improved electrical conductivity and compatibility induced by interfacial distribution of graphene, Polymer Chemistry. 4 (2013) 2939–2944. https://doi.org/10.1039/c3py00164d.

[31] Q. Meng, H.C. Kuan, S. Araby, N. Kawashima, N. Saber, C.H. Wang, J. Ma, Effect of interface modification on PMMA/graphene nanocomposites, Journal of Materials Science. 49

(2014) 5838–5849. https://doi.org/10.1007/s10853-014-8278-0.

[32] E.E. Tkalya, M. Ghislandi, G. de With, C.E. Koning, The use of surfactants for dispersing carbon nanotubes and graphene to make conductive nanocomposites, Current Opinion in Colloid and Interface Science. 17 (2012) 225–232. https://doi.org/10.1016/j.cocis.2012.03.001.

[33] R.K. Layek, A.K. Nandi, A review on synthesis and properties of polymer functionalized graphene, Polymer. 54 (2013) 5087–5103. https://doi.org/10.1016/j.polymer.2013.06.027.

[34] M. Zubair, J. Jose, A.-H. Emwas, M.A. Al-Harthi, Effect of modified graphene and microwave irradiation on the mechanical and thermal properties of poly(styrene-co-methyl methacrylate)/graphene nanocomposites, Surface and Interface Analysis. 46 (2014) 630–639. https://doi.org/10.1002/sia.5630.

[35] J. Chen, B. Yao, C. Li, G. Shi, An improved Hummers method for eco-friendly synthesis of graphene oxide, Carbon. 64 (2013) 225–229. https://doi.org/10.1016/j.carbon.2013.07.055.

[36] F. Kim, J. Luo, R. Cruz-Silva, L.J. Cote, K. Sohn, J. Huang, Self-propagating domino-like reactions in oxidized graphite, Advanced Functional Materials. 20 (2010) 2867–2873. https://doi.org/10.1002/adfm.201000736.

[37] S. Park, J. An, J.R. Potts, A. Velamakanni, S. Murali, R.S. Ruoff, Hydrazine-reduction of graphite- and graphene oxide, Carbon. (2011). https://doi.org/10.1016/j.carbon.2011.02.071.

[38] G.E. Ice, R.I. Barabash, J.W.L. Pang, Polychromatic X-ray Microdiffraction Characterization of Local Crystallographic Structure and Defect Distributions, Encyclopedia of Materials: Science and Technology. (2005) 1–15. https://doi.org/10.1016/b0-08-043152-6/02065-9.

[39] J. Li, X. Zeng, T. Ren, E. van der Heide, The preparation of graphene oxide and its derivatives and their application in bio-tribological systems, Lubricants. 2 (2014) 137–161. https://doi.org/10.3390/lubricants2030137.

[40] I. V. Krasnikova, I. V. Mishakov, A.A. Vedyagin, Functionalization, modification, and characterization of carbon nanofibers, in: Carbon-Based Nanofillers and Their Rubber Nanocomposites: Fundamentals and Applications, Elsevier Inc., 2019: pp. 75–137. https://doi.org/10.1016/B978-0-12-817342-8.00005-6.

[41] Y. Gao, O.T. Picot, E. Bilotti, T. Peijs, Influence of filler size on the properties of poly(lactic acid) (PLA)/graphene nanoplatelet (GNP) nanocomposites, European Polymer Journal. 86 (2017) 117–131. https://doi.org/10.1016/j.eurpolymj.2016.10.045.

[42] Y.S. Jun, S. Sy, W. Ahn, H. Zarrin, L. Rasen, R. Tjandra, B.M. Amoli, B. Zhao, G. Chiu, A. Yu, Highly conductive interconnected graphene foam based polymer composite, Carbon. 95

(2015) 653–658. https://doi.org/10.1016/j.carbon.2015.08.079.

[43] H. Au, N. Rubio, D.J. Buckley, C. Mattevi, M.S.P. Shaffer, Thermal Decomposition of Ternary Sodium Graphite Intercalation Compounds, Chemistry - A European Journal. 26 (2020) 6545–6553. https://doi.org/10.1002/chem.202000422.

[44] N. Rubio, H. Au, G.O. Coulter, L. Guetaz, G. Gebel, C. Mattevi, M.S.P. Shaffer, Effect of graphene flake size on functionalisation: quantifying reaction extent and imaging locus with single Pt atom tags, Chemical Science. 12 (2021) 14907–14919. https://doi.org/10.1039/d1sc01958a.

[45] L. Yan, Y. Zhou, X. Zhang, H. Zou, Y. Chen, M. Liang, Effect of graphene oxide with different exfoliation levels on the mechanical properties of epoxy nanocomposites, Polymer Bulletin. 76 (2019) 6033–6047. https://doi.org/10.1007/s00289-018-02675-x.

[46] Y. Hou, S. Lv, L. Liu, X. Liu, High-quality preparation of graphene oxide via the Hummers' method: Understanding the roles of the intercalator, oxidant, and graphite particle size, Ceramics International. 46 (2020) 2392–2402. https://doi.org/10.1016/j.ceramint.2019.09.231.

[47] Z. Zhang, H.C. Schniepp, D.H. Adamson, Characterization of graphene oxide: Variations in reported approaches, Carbon. 154 (2019) 510–521. https://doi.org/10.1016/j.carbon.2019.07.103.

[48] P. Sun, Y. Wang, H. Liu, K. Wang, D. Wu, Z. Xu, H. Zhu, Structure evolution of graphene oxide during thermally driven phase transformation: Is the oxygen content really preserved?, PLoS ONE. 9 (2014) e111908. https://doi.org/10.1371/journal.pone.0111908.

[49] P. Wick, A.E. Louw-Gaume, M. Kucki, H.F. Krug, K. Kostarelos, B. Fadeel, K.A. Dawson, A. Salvati, E. Vázquez, L. Ballerini, M. Tretiach, F. Benfenati, E. Flahaut, L. Gauthier, M. Prato, A. Bianco, Classification framework for graphene-based materials, Angewandte Chemie - International Edition. 53 (2014) 7714–7718. https://doi.org/10.1002/anie.201403335.

[50] J. Zhang, M. Zuo, X. Lv, H. Zhang, Q. Zheng, Effect of grafted graphene nanosheets on morphology evolution and conductive behavior of poly(methyl methacrylate)/poly(styrene-: Co -acrylonitrile) blends during isothermal annealing, RSC Advances. 8 (2018) 14579–14588. https://doi.org/10.1039/c8ra00439k.

[51] M.A. Pimenta, G. Dresselhaus, M.S. Dresselhaus, L.G. Cançado, A. Jorio, R. Saito, Studying disorder in graphite-based systems by Raman spectroscopy, Physical Chemistry Chemical Physics. 9 (2007) 1276–1291. https://doi.org/10.1039/b613962k.

[52] A. Kaniyoor, S. Ramaprabhu, A Raman spectroscopic investigation of graphite oxide derived graphene, AIP Advances. 2 (2012) 032183. https://doi.org/10.1063/1.4756995.

[53] V.B. Mohan, R. Brown, K. Jayaraman, D. Bhattacharyya, Characterisation of reduced graphene oxide: Effects of reduction variables on electrical conductivity, Materials Science and Engineering B: Solid-State Materials for Advanced Technology. 193 (2015) 49–60. https://doi.org/10.1016/j.mseb.2014.11.002.

[54] Q. Su, S. Pang, V. Alijani, C. Li, X. Feng, K. Müllen, Composites of craphene with large aromatic molecules, Advanced Materials. 21 (2009) 3191–3195. https://doi.org/10.1002/adma.200803808.

[55] S. Pei, H.M. Cheng, The reduction of graphene oxide, Carbon. 50 (2012) 3210–3228. https://doi.org/10.1016/j.carbon.2011.11.010.

[56] R. Krishna, D.M. Fernandes, E. Venkataramana, C. Dias, J. Ventura, C. Freire, E. Titus, P.G. Ren, D.X. Yan, X. Ji, T. Chen, Z.M. Li, C.P.P. Wong, C.W. Lai, K.M. Lee, S.B. Abd Hamid, H. Liu, X. Hu, H. Guo, J. Zhao, F. Li, D. Zhu, S. Liu, A. Thakur, S. Kumar, V.S. Rangra, A.T. Habte, D.W. Ayele, M. Hu, M.C. Ramakrishnan, R.R. Thangavelu, X. Gao, J. Jang, S. Nagase, C.K. Chua, M. Pumera, Hydrazine and Thermal Reduction of Graphene Oxide: Reaction Mechanisms, Product Structures, and Reaction Design, Chemical Communications. 52 (2015) 832–842. http://dx.doi.org/10.1039/C5CC08170J%0Ahttp://dx.doi.org/10.1016/j.matpr.2015.04.049.

[57] V.B. Mohan, K. Jayaraman, D. Bhattacharyya, Brunauer–Emmett–Teller (BET) specific surface area analysis of different graphene materials: A comparison to their structural regularity and electrical properties, Solid State Communications. 320 (2020) 114004. https://doi.org/10.1016/j.ssc.2020.114004.

[58] M.C. Kim, G.S. Hwang, R.S. Ruoff, Epoxide reduction with hydrazine on graphene: A first principles study, Journal of Chemical Physics. 131 (2009) 1–6. https://doi.org/10.1063/1.3197007.

[59] R. Muzyka, S. Drewniak, T. Pustelny, M. Chrubasik, G. Gryglewicz, Characterization of graphite oxide and reduced graphene oxide obtained from different graphite precursors and oxidized by different methods using Raman spectroscopy, Materials. 11 (2018) 15–17. https://doi.org/10.3390/ma11071050.

[60] V.B. Mohan, D. Liu, K. Jayaraman, M. Stamm, D. Bhattacharyya, Improvements in electronic structure and properties of graphene derivatives, Advanced Materials Letters. 7 (2016) 421–429. https://doi.org/10.5185/amlett.2016.6123.